the force generated by assembly of trans-SNARE complexes onto the two fusing membranes (Fig. 4), consistent with biochemical data (*23*). We postulate that after complexin binds to assembling SNARE complexes, its N-terminal sequence activates and clamps the force generated by SNARE-complex assembly. The N terminus of complexin might perform its activator function by pulling the complex closer to the membrane, possibly by binding to phospholipids, whereas the accessory N-terminal α-helix might clamp the complex by inserting into the space between the v- and t-SNAREs or even substituting for one of the SNAREs in the C-terminal segment of the trans-SNARE complex (*24*). Once anchored on the SNARE complex, the 40 N-terminal residues of complexin both activate and clamp SNARE complexes to control fast Ca^{2+}-triggered neurotransmitter release in a process that is conserved in all animals. Viewed in the broader picture, complexin and synaptotagmin therefore operate as interdependent clamp-activators of SNARE-dependent fusion, with synaptotagmin exploiting the activator effect of complexin and reversing its clamping function (*11*, *21*, *22*). In this molecular pas-de-deux, the functions of both proteins are intimately linked: Their phenotypes are identical both as activators and as clamps, and one does not operate without the other.

References and Notes

1. J. B. Sørensen, *Trends Neurosci.* **28**, 453 (2005).
2. R. Jahn, R. H. Scheller, *Nat. Rev. Mol. Cell Biol.* **7**, 631 (2006).
3. M. Verhage, R. F. Toonen, *Curr. Opin. Cell Biol.* **19**, 402 (2007).
4. M. Geppert *et al.*, *Cell* **79**, 717 (1994).
5. R. Fernandez-Chacon *et al.*, *Nature* **410**, 41 (2001).
6. M. Yoshihara, J. T. Littleton, *Neuron* **36**, 897 (2002).
7. K. Reim *et al.*, *Cell* **104**, 71 (2001).
8. X. Chen *et al.*, *Neuron* **33**, 397 (2002).
9. A. Bracher, J. Kadlec, H. Betz, W. Weissenhorn, *J. Biol. Chem.* **277**, 26517 (2002).
10. M. Xue *et al.*, *Nat. Struct. Mol. Biol.* **14**, 949 (2007).
11. C. G. Giraudo, W. S. Eng, T. J. Melia, J. E. Rothman, *Science* **313**, 676 (2006), published online 22 June 2006; 10.1126/science.1129450.
12. C. G. Giraudo *et al.*, *J. Biol. Chem.* **283**, 21211 (2008).
13. J. R. Schaub, X. Lu, B. Doneske, Y. K. Shin, J. A. McNew, *Nat. Struct. Mol. Biol.* **13**, 748 (2006).
14. T. Y. Yoon *et al.*, *Nat. Struct. Mol. Biol.* **15**, 707 (2008).
15. S. Huntwork, J. T. Littleton, *Nat. Neurosci.* **10**, 1235 (2007).
16. K. Weninger, M. E. Bowen, U. B. Choi, S. Chu, A. T. Brunger, *Structure* **16**, 308 (2008).
17. R. Guan, H. Dai, J. Rizo, *Biochemistry* **47**, 1474 (2008).
18. S. Schoch *et al.*, *Science* **294**, 1117 (2001).
19. Single-letter abbreviations for the amino acid residues are as follows: A, Ala; C, Cys; D, Asp; E, Glu; F, Phe; G, Gly; H, His; I, Ile; K, Lys; L, Leu; M, Met; N, Asn; P, Pro; Q, Gln; R, Arg; S, Ser; T, Thr; V, Val; W, Trp; and Y, Tyr.
20. For a description of the experimental procedures, see the supporting online material.
21. J. Tang *et al.*, *Cell* **126**, 1175 (2006).
22. A. Maximov, T. C. Südhof, *Neuron* **48**, 547 (2005).
23. K. Hu, J. Carroll, C. Rickman, B. Davletov, *J. Biol. Chem.* **277**, 41652 (2002).
24. C. G. Giraudo *et al.*, *Science* **323**, 512 (2009).

25. We thank J. Rizo and L. Chen for advice and critical comments. This study was supported by an investigatorship to T.C.S. from the Howard Hughes Medical Institute.

Supporting Online Material

www.sciencemag.org/cgi/content/full/323/5913/516/DC1
SOM Text
Figs. S1 to S14
Table S1
References

29 September 2008; accepted 5 December 2008
10.1126/science.1166505

Widespread Increase of Tree Mortality Rates in the Western United States

Phillip J. van Mantgem,[1]*†‡ Nathan L. Stephenson,[1]*† John C. Byrne,[2] Lori D. Daniels,[3] Jerry F. Franklin,[4] Peter Z. Fulé,[5] Mark E. Harmon,[6] Andrew J. Larson,[4] Jeremy M. Smith,[7] Alan H. Taylor,[8] Thomas T. Veblen[7]

Persistent changes in tree mortality rates can alter forest structure, composition, and ecosystem services such as carbon sequestration. Our analyses of longitudinal data from unmanaged old forests in the western United States showed that background (noncatastrophic) mortality rates have increased rapidly in recent decades, with doubling periods ranging from 17 to 29 years among regions. Increases were also pervasive across elevations, tree sizes, dominant genera, and past fire histories. Forest density and basal area declined slightly, which suggests that increasing mortality was not caused by endogenous increases in competition. Because mortality increased in small trees, the overall increase in mortality rates cannot be attributed solely to aging of large trees. Regional warming and consequent increases in water deficits are likely contributors to the increases in tree mortality rates.

As key regulators of global hydrologic and carbon cycles, forests are capable of contributing substantial feedbacks to global changes (*1*). Such feedbacks may already be under way; for example, forest carbon storage may be responding to environmentally driven changes in global patterns of tree growth and forest productivity (*2*–*4*). Recent warming has been implicated as contributing to episodes of forest dieback (pulses of greatly elevated tree mortality), such as those mediated by bark beetle outbreaks in western North America (*5*, *6*). Yet little effort has gone toward determining whether environmental changes are contributing to chronic, long-term changes in tree demographic rates (mortality and recruitment). Changes in demographic rates, when compounded over time, can alter forest structure, composition, and function (*7*). For example, a persistent doubling of background mortality rate (such as from 1 to 2% $year^{-1}$) ultimately would cause a >50% reduction in average tree age in a forest, and hence a potential reduction in average tree size. Additionally, changing demographic rates could indicate forests approaching thresholds for abrupt dieback. Yet spatially extensive analyses of long-term changes in tree demographic rates have been limited to tropical forests, where mortality and recruitment rates both have increased over the past several decades, perhaps in response to rising atmospheric CO_2 concentrations, nutrient deposition, or other environmental changes (*2*, *8*). Comparably extensive analyses have not been conducted in temperate forests.

We sought to determine whether systematic changes in tree demographic rates have occurred recently in coniferous forests of the western United States, and if so, to identify possible causes of those changes. Although the western United States has witnessed recent episodes of forest dieback related to bark beetle outbreaks or combinations of drought and outbreaks (*5*, *6*), most forested land continues to support seemingly healthy forests that have not died back (*9*). To minimize transient dynamics associated with stand development and succession, we limited our analyses to data from repeated censuses in undisturbed forest stands more than 200 years old (*10*). Old forests contain trees of all ages and sizes (*11*, *12*), and any large, persistent changes in demographic rates over a short period (such as a few decades) are likely to be consequences of exogenous environmental changes (*2*, *13*). In contrast, in young forests rapid demographic changes can sometimes result largely from endogenous processes (such as self-thinning during stand development) (*14*), potentially obscuring environmentally driven changes.

[1]U.S. Geological Survey, Western Ecological Research Center, Three Rivers, CA 93271, USA. [2]USDA Forest Service, Rocky Mountain Research Station, Moscow, ID 83843, USA. [3]Department of Geography, University of British Columbia, Vancouver, British Columbia V6T IZ2, Canada. [4]College of Forest Resources, University of Washington, Seattle, WA 98195, USA. [5]School of Forestry and Ecological Restoration Institute, Northern Arizona University, Flagstaff, AZ 86011, USA. [6]Department of Forest Science, Oregon State University, Corvallis, OR 97331, USA. [7]Department of Geography, University of Colorado, Boulder, CO 80309, USA. [8]Department of Geography, Pennsylvania State University, University Park, PA 16802, USA.

*These authors contributed equally to this work.
†To whom correspondence should be addressed. E-mail: pvanmantgem@usgs.gov (P.J.V.); nstephenson@usgs.gov (N.L.S.)
‡Present address: U.S. Geological Survey, Western Ecological Research Center, Arcata, CA 95521, USA.

Seventy-six long-term forest plots from three broad regions, spanning 14° of latitude and 18° of longitude and at elevations of 130 to 3353 m (Fig. 1 and table S1), met our criteria for analysis (*10*). Plots ranged from 0.25 to 15.75 ha ($\bar{x}$ = 1.33 ha), collectively containing 58,736 living trees over the study period, of which 11,095 died. The plots were originally established for diverse purposes—such as to investigate different stages of forest development, document dynamics of certain forest types, explore forest dynamics along environmental gradients, or act as controls for silvicultural experiments [see references in (*10*)]—that are unlikely to produce bias relative to our study's goals. We analyzed data from 1955 and later; only five plots from one region had earlier censuses. For individual plots, the initial census year analyzed ranged from 1955 to 1994 ($\bar{x}$ = 1981); the final census year ranged from 1998 to 2007 ($\bar{x}$ = 2004). Plots were censused three to seven times ($\bar{x}$ = 4.8). Our generally conservative estimates of forest ages at the time of initial censuses averaged ~450 years, with some plots exceeding 1000 years.

We used generalized nonlinear models to regress demographic rates on year; generalized nonlinear mixed models (GNMMs) were used when several plots were analyzed collectively (*10*). Demographic rates were estimated by annual compounding over the census interval length. All parameters were estimated by maximum likelihood.

Our models showed that mortality rates increased in 87% of plots (Fig. 1) ($P < 0.0001$, two-tailed binomial test). Mortality rate increased significantly for all plots combined and in each of the three regions (Fig. 2 and Table 1), with estimated doubling periods ranging from 17 years (Pacific Northwest) to 29 years (interior). Mortality rates also increased at low, middle, and high elevations (<1000 m, 1000 to 2000 m, and >2000 m, respectively) and for small, medium, and large trees (stem diameter <15 cm, 15 to 40 cm, and >40 cm, respectively) (Fig. 2 and Table 1). The three most abundant tree genera in our plots (comprising 77% of trees) are dominated by different life history traits (*Tsuga*, late successional; *Pinus*, generally shade-intolerant; *Abies*, generally shade-tolerant); all three showed increasing mortality rates (Fig. 2 and Table 1). An introduced fungal pathogen, *Cronartium ribicola*, is known to contribute to increasing mortality rates in five-needled species of *Pinus* (*15*). When all five-needled *Pinus* were removed from analysis, mortality rates among the remaining *Pinus* (those immune to the pathogen) still increased [$a = 0.027$, $P = 0.0011$, GNMM, $n = 22$, where a is the estimated annual fractional change in mortality rate; see (*10*)]. Finally, trees belonging to the remaining 16 genera (23% of all trees) collectively showed increasing mortality rates (Fig. 2 and Table 1).

In contrast to mortality rates, recruitment rates increased in only 52% of plots—a proportion indistinguishable from random ($P = 0.80$, two-tailed binomial test). There was no detectable trend in recruitment for all plots combined, nor when regions were analyzed separately ($P \geq 0.20$, GNMM; table S2).

We examined three classes of possible causes of the increasing tree mortality rates: methodological artifacts, endogenous processes, and exogenous processes. We tested for and ruled out several obvious potential sources of methodological artifacts (*10*). Among endogenous processes, perhaps the best-known cause of increasing tree mortality rates is increasing competition resulting from increasing forest density and basal area (*11*, *12*). Such changes might especially be expected in the subset of old forests in the western United States that formerly experienced frequent surface fires; in these forests, fire exclusion (generally spanning the last century) often resulted in an initial increase in forest density and basal area (*16*, *17*). However, consistent with our observations of increasing mortality without compensating increases in recruitment, forest density and basal area declined slightly during the study period

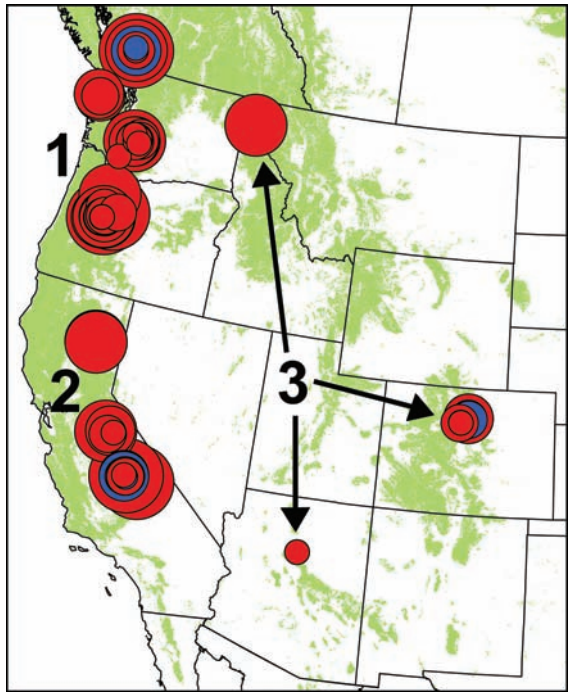

Fig. 1. Locations of the 76 forest plots in the western United States and southwestern British Columbia. Red and blue symbols indicate, respectively, plots with increasing or decreasing mortality rates. Symbol size corresponds to annual fractional change in mortality rate (smallest symbol, <0.025 year^{-1}; largest symbol, >0.100 year^{-1}; the three intermediate symbol sizes are scaled in increments of 0.025 year^{-1}). Numerals indicate groups of plots used in analyses by region: (1) Pacific Northwest, (2) California, and (3) interior. Forest cover is shown in green.

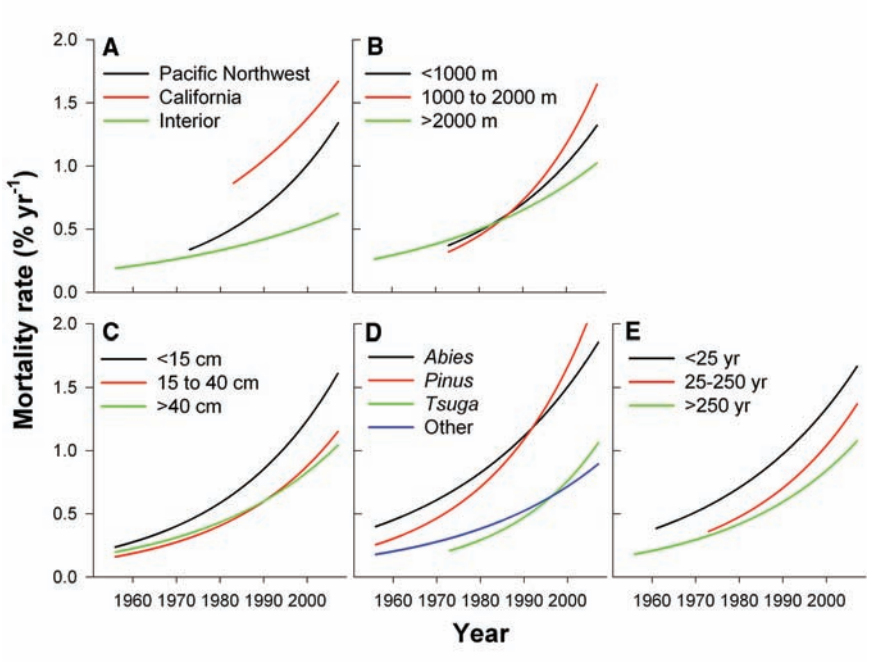

Fig. 2. Modeled trends in tree mortality rates for (**A**) regions, (**B**) elevational class, (**C**) stem diameter class, (**D**) genus, and (**E**) historical fire return interval class.

[$P \leq 0.028$, linear mixed model (LMM); fig. S1]. Thus, forest structural changes are consistent with a slight decline rather than an increase in potential for competition over the study period, which suggests that increasing mortality rates cannot be attributed to changes in forest structure.

Fire exclusion conceivably could affect mortality rates through mechanisms unrelated to forest structural changes, such as allowing increases in insects or pathogens that were formerly controlled by fire. We therefore classified plots by their pre–fire exclusion fire return intervals: short, intermediate, and long (<25 years, 25 to 250 years, and >250 years, respectively) (table S1). If fire exclusion ultimately were responsible for increasing tree mortality rates, we would expect to see increases in plots with historically short fire return intervals (which have experienced substantial recent changes in fire regime) and little or no change in mortality rates in plots with historically long return intervals (which have experienced little or no change in fire regime). However, mortality rates showed comparable increases in each of the three classes (Fig. 2 and Table 1); we therefore conclude that fire exclusion is an unlikely cause of the observed increases in mortality rates.

Mortality rates could increase if a cohort of old trees begins to die and fall, crushing smaller trees at an increasing rate [a mechanism related to the proposed "majestic forest" effect; see references in (*8*)]. If such a mechanism were responsible for the observed increase in tree mortality rates, we would expect to see no parallel increase in mortality rates of small trees that died standing (i.e., trees <15 cm in diameter that died of causes other than being crushed by falling trees from an aging cohort), because such deaths are independent of deaths in an aging cohort. However, the mortality rate of small trees that died standing increased rapidly in recent decades, doubling in ~16 years ($P < 0.0001$, GNMM; table S3); thus, other mechanisms must be acting. Finally, mortality rates increased in all major genera rather than being limited to those dominated by a particular life history trait (such as shade intolerance), which suggests that successional dynamics are unlikely to be primary drivers of increasing mortality rates.

We conclude that endogenous processes are unlikely to be major contributors to the observed rapid, synchronous doubling of mortality rates in our heterogeneous sample of old forests at a subcontinental scale. Moreover, the available evidence is inconsistent with major roles for two possible exogenous causes: forest fragmentation and air pollution (*10*).

We suggest that regional warming may be the dominant contributor to the increases in tree mortality rates. From the 1970s to 2006 (the period including the bulk of our data; table S1), the mean annual temperature of the western United States increased at a rate of 0.3° to 0.4°C decade^{-1}, even approaching 0.5°C decade^{-1} at the higher elevations typically occupied by forests (*18*). This regional warming has contributed to widespread hydrologic changes, such as declining fraction of precipitation falling as snow (*19*), declining snowpack water content (*20*), earlier spring snowmelt and runoff (*21*), and a consequent lengthening of the summer drought (*22*). Specific to our study sites, mean annual precipitation showed no directional trend over the study period ($P = 0.62$, LMM), whereas both mean annual temperature and climatic water deficit (annual evaporative demand that exceeds available water) increased significantly ($P < 0.0001$, LMM) (*10*). Furthermore, temperature and water deficit were positively correlated with tree mortality rates ($P \leq 0.0066$, GNMM; table S4).

Warming could contribute to increasing mortality rates by (i) increasing water deficits and thus drought stress on trees, with possible direct and indirect contributions to tree mortality (*13*, *23*); (ii) enhancing the growth and reproduction of insects and pathogens that attack trees (*6*); or (iii) both. A contribution from warming is consistent with both the apparent role of warming in episodes of recent forest dieback in western North America (*5*, *6*) and the positive correlation between short-term fluctuations in background mortality rates and climatic water deficits observed in California and Colorado (*13*, *24*).

The rapid and pervasive increases in tree mortality rates in old forests of the western United States are notable for several reasons. First, increasing mortality rates could presage substantial changes in forest structure, composition, and function (*7*, *25*), and in some cases could be symptomatic of forests that are stressed and vulnerable to abrupt dieback (*5*). Indeed, since their most recent censuses, several of our plots in the interior region experienced greatly accelerated mortality due to bark beetle outbreaks, and in some cases nearly complete mortality of large trees (*10*). Second, the increasing mortality rates demonstrate that ongoing, subcontinental-scale changes in tree demographic rates are not limited to the tropics (*8*). Third, some of the changes in the western United States contrast sharply with those in the tropics, where increasing mortality rates have been paralleled by increasing recruitment rates and basal area (*2*, *8*). In the western United States, recruitment rates have not changed while forest density and basal area have declined slightly. Fourth, our results are inconsistent with a major role for endogenous causes of increasing mortality rates. Instead, the evidence is consistent with contributions from exogenous causes, with regional warming and consequent drought stress being the most likely drivers.

Table 1. Fixed effects of generalized nonlinear mixed models describing mortality rate trends (*10*); *a* is the estimated annual fractional change in mortality rate (*10*) and *n* is the number of forest plots used in the model.

Model	Data	*a*	SE	*P*	*n*
Mortality trend	All plots	0.039	0.005	<0.0001	76
Mortality trend by region	Pacific Northwest	0.042	0.006	<0.0001	47
	California	0.028	0.009	0.0050	20
	Interior	0.024	0.009	0.0319	9
Mortality trend by elevation class	<1000 m	0.038	0.007	<0.0001	33
	1000 to 2000 m	0.050	0.010	<0.0001	20
	>2000 m	0.027	0.006	0.0003	23
Mortality trend by stem diameter class	<15 cm	0.039	0.006	<0.0001	61
	15 to 40 cm	0.040	0.006	<0.0001	76
	>40 cm	0.033	0.007	<0.0001	76
Mortality trend by genus	*Abies*	0.031	0.010	0.0025	62
	Pinus	0.044	0.010	<0.0001	37
	Tsuga	0.049	0.009	<0.0001	47
	All other genera	0.032	0.008	<0.0001	64
Mortality trend by fire return interval	<25 years	0.033	0.008	0.0009	15
	25 to 250 years	0.040	0.006	<0.0001	32
	>250 years	0.036	0.010	0.0008	29

References and Notes

1. G. B. Bonan, *Science* **320**, 1444 (2008).
2. S. L. Lewis *et al.*, *Philos. Trans. R. Soc. London Ser. B* **359**, 421 (2004).
3. A. S. Jump, J. M. Hunt, J. Peñuelas, *Glob. Change Biol.* **12**, 2163 (2006).
4. K. J. Feeley, S. J. Wright, M. N. Nur Supardi, A. R. Kassim, S. J. Davies, *Ecol. Lett.* **10**, 461 (2007).
5. D. D. Breshears *et al.*, *Proc. Natl. Acad. Sci. U.S.A.* **102**, 15144 (2005).
6. K. F. Raffa *et al.*, *Bioscience* **58**, 501 (2008).
7. R. K. Kobe, *Ecol. Monogr.* **66**, 181 (1996).
8. O. L. Phillips *et al.*, *Philos. Trans. R. Soc. London Ser. B* **359**, 381 (2004).
9. J. A. Hicke, J. C. Jenkins, D. S. Ojima, M. Ducey, *Ecol. Appl.* **17**, 2387 (2007).
10. See supporting material on *Science* Online.
11. C. D. Oliver, B. C. Larson, *Forest Stand Dynamics* (McGraw-Hill, New York, 1990).
12. J. F. Franklin *et al.*, *For. Ecol. Manage.* **155**, 399 (2002).
13. P. J. van Mantgem, N. L. Stephenson, *Ecol. Lett.* **10**, 909 (2007).
14. J. A. Lutz, C. B. Halpern, *Ecol. Monogr.* **76**, 257 (2006).
15. G. I. McDonald, R. J. Hoff, in *Whitebark Pine Communities*, D. F. Tomback, S. F. Arno, R. E. Keane, Eds. (Island Press, Washington, DC, 2001), pp. 193–220.
16. R. T. Brown, J. K. Agee, J. F. Franklin, *Conserv. Biol.* **18**, 903 (2004).
17. M. North, J. Innes, H. Zald, *Can. J. For. Res.* **37**, 331 (2007).
18. H. F. Diaz, J. K. Eischeid, *Geophys. Res. Lett.* **34**, L18707 (2007).

19. N. Knowles, M. D. Dettinger, D. R. Cayan, *J. Clim.* **19**, 4545 (2006).
20. P. W. Mote, A. F. Hamlet, M. P. Clark, D. P. Lettenmaier, *Bull. Am. Meteorol. Soc.* **86**, 39 (2005).
21. I. T. Stewart, D. R. Cayan, M. D. Dettinger, *J. Clim.* **18**, 1136 (2005).
22. A. L. Westerling, H. G. Hidalgo, D. R. Cayan, T. W. Swetnam, *Science* **313**, 940 (2006); published online 5 July 2006 (10.1126/science.1128834).
23. N. McDowell *et al*., *New Phytol.* **178**, 719 (2008).
24. C. Bigler, D. G. Gavin, C. Gunning, T. T. Veblen, *Oikos* **116**, 1983 (2007).
25. A. W. Fellows, M. L. Goulden, *Geophys. Res. Lett.* **35**, L12404 (2008).

26. We thank the many people involved in establishing and maintaining the permanent forest plots; C. Allen, A. Das, J. Halofsky, J. Hicke, J. Lutz, and four anonymous reviewers for helpful comments on the manuscript; and J. Yee for essential statistical advice. The forest plots were funded by NSF's Long-term Studies Program (DEB-0218088); the Wind River Canopy Crane Program through cooperative agreement PNW 08-DG-11261952-488 with the USDA Forest Service Pacific Northwest Research Station; various awards through the USDA Forest Service's Pacific Northwest, Pacific Southwest, and Rocky Mountain research stations and the McIntire-Stennis Cooperative Forestry Program; NSF awards DEB-0743498 and BCS-0825823; the Natural Science and Engineering Research Council of Canada; and various awards through the U.S. National Park Service and U.S. Geological Survey (USGS). This work is a contribution of the Western Mountain Initiative (a USGS global change research project) and the Cordillera Forest Dynamics Network (CORFOR).

Supporting Online Material

www.sciencemag.org/cgi/content/full/323/5913/521/DC1
Materials and Methods
SOM Text
Figs. S1 to S6
Tables S1 to S4
References

22 August 2008; accepted 3 December 2008
10.1126/science.1165000

The Sphingolipid Transporter Spns2 Functions in Migration of Zebrafish Myocardial Precursors

Atsuo Kawahara,[1,2]* Tsuyoshi Nishi,[3,4] Yu Hisano,[3,4] Hajime Fukui,[1] Akihito Yamaguchi,[3,4] Naoki Mochizuki[1]

Sphingosine-1-phosphate (S1P) is a secreted lipid mediator that functions in vascular development; however, it remains unclear how S1P secretion is regulated during embryogenesis. We identified a zebrafish mutant, *ko157*, that displays cardia bifida (two hearts) resembling that in the *S1P receptor-2* mutant. A migration defect of myocardial precursors in the *ko157* mutant is due to a mutation in a multipass transmembrane protein, Spns2, and can be rescued by S1P injection. We show that the export of S1P from cells requires Spns2. *spns2* is expressed in the extraembryonic tissue yolk syncytial layer (YSL), and the introduction of *spns2* mRNA in the YSL restored the cardiac defect in the *ko157* mutant. Thus, Spns2 in the YSL functions as a S1P transporter in S1P secretion, thereby regulating myocardial precursor migration.

During the late stages of zebrafish segmentation characterized by the formation of the somites, the myocardial precursors from both sides of the anterior lateral plate mesoderm migrate toward the midline to form the heart tube (*1*, *2*). Forward genetic analysis in zebrafish has helped to uncover genes involved in vertebrate heart formation (*3*). To identify additional regulators of heart development, we performed *N*-ethyl-*N*-nitrosourea (ENU) mutagenesis screening for mutations specifically affecting cardiac morphogenesis. We isolated a recessive *ko157* mutant that displayed two hearts, a condition known as cardia bifida with swollen pericardial sacs (Fig. 1, A, B, E, and F). The expression of myocardial markers [*nkx2.5* and *cardiac myosin light chain 2* (*cmlc2*)] and chamber-specific markers [*atrial myosin heavy chain* (*amhc*) and *ventricular myosin heavy chain* (*vmhc*)] was detected in two separated domains (Fig. 1, C and G, and fig. S2); this finding suggests that the myocardial precursors failed to migrate but differentiated into two chambers at the bilateral positions.

The migration of several mesodermal derivatives examined by the expression pattern of a vascular marker (*fli1*), an erythroid marker (*gata1*), a pronephric marker (*pax2*), and a lateral plate mesoderm marker (*hand2*) was not impaired in *ko157* mutants (figs. S2 and S3), which suggests that the migration of myocardial precursors is dominantly affected. Besides cardia bifida, there were abnormal blisters at the tip of the tail in the mutant (Fig. 1, D and H). These two characteristic phenotypes (cardia bifida and tail blisters) in the *ko157* mutant were similar to those in the *miles apart* (*mil*)/*S1P receptor-2* (*S1P2*) mutant (*4*). Sphingosine-1-phosphate (S1P) is a lipid mediator involved in cell growth, death, migration, and differentiation (*5*–*8*). Both cardia bifida and tail blisters were observed in embryos injected with an antisense morpholino for *mil/S1P2* (*mil* MO; 15 ng) (*9*) (fig. S4 and table S1), suggesting a genetic interaction between *ko157* and *mil/S1P2*.

Genetic mapping of the *ko157* mutation by means of simple sequence length polymorphism

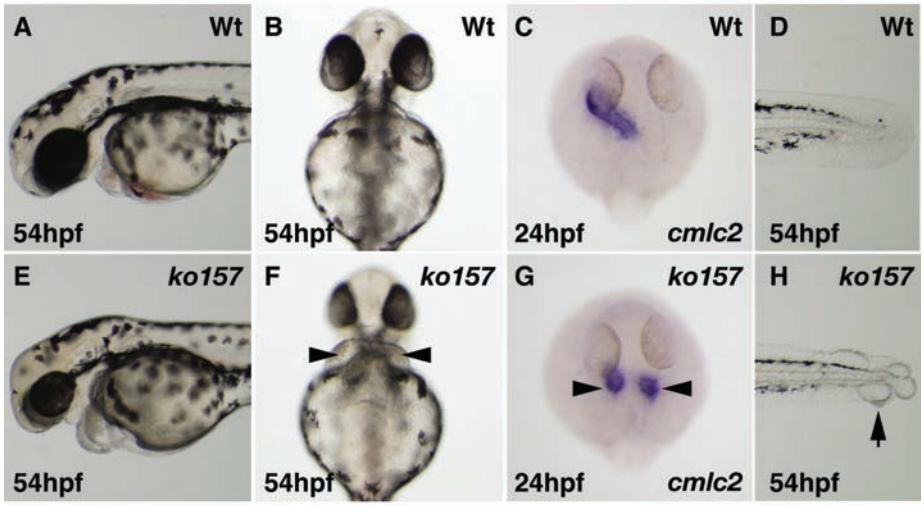

Fig. 1. Morphological phenotypes of *ko157* mutants. (**A**, **B**, **D**, **E**, **F**, and **H**) Stereomicroscopic views of wild-type (Wt) embryo [(A), (B), and (D)] and *ko157* mutant [(E), (F), and (H)]. Two swollen pericardial sacs (arrowheads) at 54 hours post-fertilization (hpf) were observed in *ko157* mutant [(E) and (F)] but not in Wt embryos [(A) and (B)]. (B) and (F) are ventral views. (**C** and **G**) Two hearts (arrowheads) in *ko157* mutants at 24 hpf were visualized (dorsal view) by whole-mount in situ hybridization with antisense *cmlc2* probe. *ko157* mutant (H), but not Wt embryos (D), exhibited tail blisters (arrow).

[1]Department of Structural Analysis, National Cardiovascular Center Research Institute, Fujishirodai 5-7-1, Suita, Osaka 565-8565, Japan. [2]HMRO, Kyoto University Faculty of Medicine, Yoshida, Sakyo-Ku, Kyoto 606-8501, Japan. [3]Department of Cell Membrane Biology, Institute of Scientific and Industrial Research, Osaka University, 8-1 Mihogaoka, Ibaraki-shi, Osaka 567-0047, Japan. [4]Graduate School of Pharmaceutical Sciences, Osaka University, Suita-shi, Osaka 565-0871, Japan.

*To whom correspondence should be addressed. E-mail: atsuo@ri.ncvc.go.jp